Bioorganic & Medicinal Chemistry 17 (2009) 326–336

Contents lists available at ScienceDirect

Bioorganic & Medicinal Chemistry

journal homepage: www.elsevier.com/locate/bmc

Synthesis and biological activity of 1,4-dihydrobenzothiopyrano[4,3-*c*]pyrazole derivatives, novel pro-apoptotic mitochondrial targeted agents

L. Dalla Via [a], A. M. Marini [b,*], S. Salerno [b], C. La Motta [b], M. Condello [c], G. Arancia [c], E. Agostinelli [d], A. Toninello [e]

[a] *Department of Pharmaceutical Sciences, University of Padova, Via Marzolo 5, 35131 Padova, Italy*
[b] *Department of Pharmaceutical Sciences, University of Pisa, Via Bonanno 6, 56126 Pisa, Italy*
[c] *Department of Technology and Health, Istituto Superiore di Sanità, Rome, Italy*
[d] *Department of Biochemical Sciences, Institute of Molecular Biology and Pathology, University of Rome "La Sapienza" and CNR, Rome, Italy*
[e] *Department of Biological Chemistry, University of Padova, Via G. Colombo 3, 35121 Padova, Italy*

ARTICLE INFO

Article history:
Received 24 April 2008
Revised 27 October 2008
Accepted 30 October 2008
Available online 5 November 2008

Keywords:
Dihydrobenzothiopyranopyrazole
Antiproliferative activity
Mitochondria
Reactive oxygen species
Permeability transition

ABSTRACT

This study reports the synthesis of a number of 1- and 2-phenyl derivatives of the 1,4-dihydrobenzothiopyrano[4,3-*c*]pyrazole nucleus, which were obtained by the reaction of the versatile 7-substituted 2,3-dihydro-3-hydroxymethylene-4*H*-1-benzothiopyran-4-ones with hydrazine and substituted phenylhydrazines. The antiproliferative activity of the synthesized compounds was evaluated by an in vitro assay on human tumor cell lines (HL-60 and HeLa) and showed a significant capacity of the 7-methoxy-substituted benzothiopyrano[4,3-*c*]pyrazoles **3b–d**, carrying the pendant phenyl group in the 1-position, to inhibit cell growth. Investigation of the mechanism of action indicated the induction of the mitochondrial permeability transition (MPT) as the molecular event responsible for the inhibition of cell growth. This phenomenon is related to the ability of the test compounds to cause a rapid Ca^{2+}-dependent and cyclosporin A-sensitive collapse of the transmembrane potential ($\Delta\Psi$) and matrix swelling. All this leads to the release of caspase activators, such as cytochrome *c* (cyt *c*) and apoptosis-inducing factor (AIF), which trigger the pro-apoptotic pathway leading to DNA fragmentation.

1. Introduction

In the development of new anticancer agents, the central role of mitochondria in mediating programmed cell death has raised a large amount of interest due to their key implications in many pathways essential to both the life and death of cells.[1,2] These organelles play a central role in the integration of pro- and anti-apoptotic stimuli. In addition, direct targeting of mitochondrial functions appears to be of significant therapeutic relevance, since it is known that inadequate apoptosis leads to over-proliferation of cells and that the rapid and continuous growth of tumor cells is highly energy-dependent.

Some mitochondrial deregulations have been described as the hallmarks of apoptosis; among them a central role is played by the induction of the mitochondrial membrane permeability transition (MPT), a process that leads to an increase in the inner membrane's permeability to solutes with a molecular mass up to 1500 Da.[3] This phenomenon is regulated by the opening of a large conductance channel known as the permeability transition pore. Opening of this non-selective pore provokes the dissipation of the inner transmembrane potential ($\Delta\Psi$), matrix swelling, and outer membrane disruption, thus leading to the release of a caspase activator, such as cytochrome *c* (cyt *c*), which triggers the pro-apoptotic pathway leading to DNA fragmentation.

In this regard, it has to be emphasized that a primary insult, such as a DNA adduct, that takes place after chemotherapy can cause apoptotic cell death. In particular, in the absence of DNA repair, an increase in level of p53 occurs. This pro-apoptotic protein induces an increase in the level of Bax, a mammalian cell death protein targeting mitochondrial membranes, which moves to the mitochondria and causes the release of cyt *c*. Once in the cytoplasm, cyt *c* interacts with additional proteins to form the so-called 'apoptosome'. The apoptosome implies the participation, besides cyt *c*, of APAF-1 (which binds ATP) and caspase-9, which together activate another component, pro-caspase-3. This, in turn, induces the activation of caspase-3, which cleaves and activates DNA fragmentation factors (DFF) that subsequently activate endonucleases. Together, these steps produce the biochemical and morphological changes in the cell that are collectively recognized as apoptosis.[4,5]

Interestingly, certain conventional, clinically used anticancer drugs have shown a direct and in some cases specific action on mitochondria in addition to their cytosolic or nuclear effects. Indeed, it is well established that the cardiotoxicity and the

* Corresponding author. Tel.: +39 0502219555; fax: +39 0502219605.
E-mail address: marini@farm.unipi.it (A.M. Marini).

0968-0896/$ - see front matter © 2008 Elsevier Ltd. All rights reserved.
doi:10.1016/j.bmc.2008.10.067

occurrence of multidrug resistance (MDR) of Anthracenediones and Anthracyclines have been attributed to their accumulation in the mitochondrial lipid membrane and subsequent redox activity of the quinone moiety.[6–10] Some Topoisomerase II-targeting anticancer drugs such as Etoposide or Amsacrine, have demonstrated the capacity to interact with mitochondrial functions, also with a mechanism related to the permeability transition pore formation.[11–13] However, most of the current anticancer drugs do not directly target mitochondria but must first damage other molecular targets to generate the signals that, subsequently, trigger the mitochondrial pathway of apoptosis. These observations support the search for compounds that are able to affect mitochondrial functions, in order to develop novel anticancer derivatives endowed with low DNA damaging properties and the ability to retain efficacy in MDR tumor cells.

As a part of our research program devoted to the preparation and evaluation of new antiproliferative agents, we extensively studied several polycyclic chromophores[14–16] among which we recently disclosed that the 2-amino-5*H*-pirido[3′,2′:5,6]thiopyrano[4,3-*d*]pyrimidine (PTP) **I**[17] showed a detectable cytotoxic activity on two human tumor cell lines (HeLa and HL-60) which was ascribed to its ability to interfere with mitochondrial functions.

With the aim to identify novel active compounds, we carried out a number of modifications on the structure of **I**, first obtaining the isosteric derivative **II** (R = NH_2)[18] which was devoid of any activity; we then substituted the polar amino group with a phenyl one, to give **II** (R = C_6H_5), which showed an appreciable cytotoxic activity on HL-60 cell line (IC_{50} = 7.15 μM).[18]

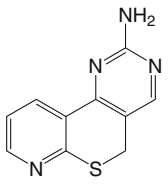

I

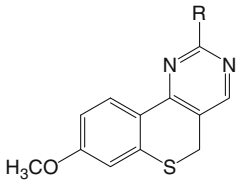

II

R = NH_2, C_6H_5

In this paper, we describe the synthesis of the benzothiopyrano[4,3-*d*]pyrazoles **III**, in which the pyrazole moiety gave us the potential to insert a pendant phenyl ring both in the 1- and in the 2-position of the chromophore.

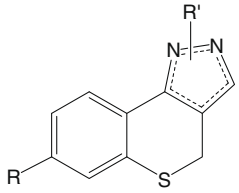

III

R = OCH_3, Cl

R' = H, C_6H_5, *p*-Cl-C_6H_4, *p*-OCH_3-C_6H_4

The antiproliferative activity of the new derivatives **III** was evaluated on two human tumor cell lines (HL-60 and HeLa); then, the ability to induce MPT on isolated rat liver mitochondria via an oxidative stress is discussed. Moreover, the release of cyt *c* and AIF by mitochondria and the occurrence of apoptosis on HeLa cells were demonstrated. Finally, to correlate the induction of MPT with the antiproliferative activity, the effect of cyclosporin A (CsA) and the mitochondrial membrane potential on HeLa cells were investigated.

2. Results and discussion

2.1. Chemistry

The preparation of the benzothiopyranopyrazoles and the 1-aryl substituted derivatives was performed following the synthetic route described in Scheme 1. The starting key 7-methoxy- or 7-chloro-3-hydroxymethylenebenzothiopyranones (**1** and **2)** were obtained reacting, in toluene solution, ethyl formate with the suitable 7-methoxy- or 7-chloro-2,3-dihydrobenzo[3′,2′:5,6]thiopyran-4(4*H*)-one, which were prepared following a previously described procedure.[19]

The condensation of compounds **1** and **2**, containing the reactive methine group adjacent to the C=O function, with hydrazine or the appropriate phenylhydrazine hydrochlorides afforded the target series **3a–d** and **4a–d**.

The physicochemical properties and purity of the final compounds were assessed by TLC and analytical and ^{1}H NMR spectral data; the resultant assignment values are in accordance with the structures proposed and with our previously reported results.[20,21]

The synthetic sequence leading to the 2-phenyl substituted 1,4-dihydrobenzo thiopyrano[4,3-*c*]pyrazoles (Scheme 2) involved the conversion of the 3-hydroxymethylene compound **1** into the intermediate *p*-toluensulfonate **5**, in which the reactive methine functionality was protected as previously reported by us.[21] The subsequent condensation of **5** with the appropriate phenylhydrazine hydrochloride, in anhydrous dimethylformamide at room temperature, involves, as a first step, only the carbonylic function in the 4-position, affording the intermediate arylhydrazones.[21] These intermediates easily cyclize in situ by heating (100 °C) the reaction mixture, thus affording the desired 2-substituted derivatives **6b–d**. The compounds were purified by flash chromatography and characterized by analytical and spectral data. In particular, the most discriminating feature of the ^{1}H NMR spectra of compounds **6b–d** was a singlet at ≈8.3 ppm attributed to the proton in the 3-position of the pyrazole moiety, while the same proton of the analogous 1-aryl substituted compounds **3b–d** resonated at ≈7.6 ppm.

2.2. Antiproliferative activity

The antiproliferative activity of the new benzothiopyranopyrazole derivatives was evaluated on two human tumor cell lines, HeLa (cervix adenocarcinoma cells) and HL-60 (myeloid leukemic cells), and was expressed as IC_{50} values, that is, the concentration (μM) of the compound causing 50% of cell death with respect to the control culture (Table 1).

The results indicated the occurrence of a significant antiproliferative effect for derivatives **3b–d**, which were characterized by the presence of a methoxy substituent in position 7 and a pendant phenyl, *p*-chlorophenyl or *p*-methoxyphenyl at the 1-position of the heterocyclic moiety, respectively. In particular, **3c** appeared to be the most active compound in both cell lines, showing IC_{50} values in the low micromolar range. Interestingly, the parent compound **3a**, lacking the phenyl side group, was unable to exert any cytotoxic effect; the same effect was also true for the derivatives **6b–d**, which differ from **3b–d** in the position of the phenyl side group on the pyrazole ring. Thus, to exert a significant antiproliferative effect, the benzothiopyranopyrazole moiety requires the presence of a phenyl group, preferably *p*-chloro substituted, linked

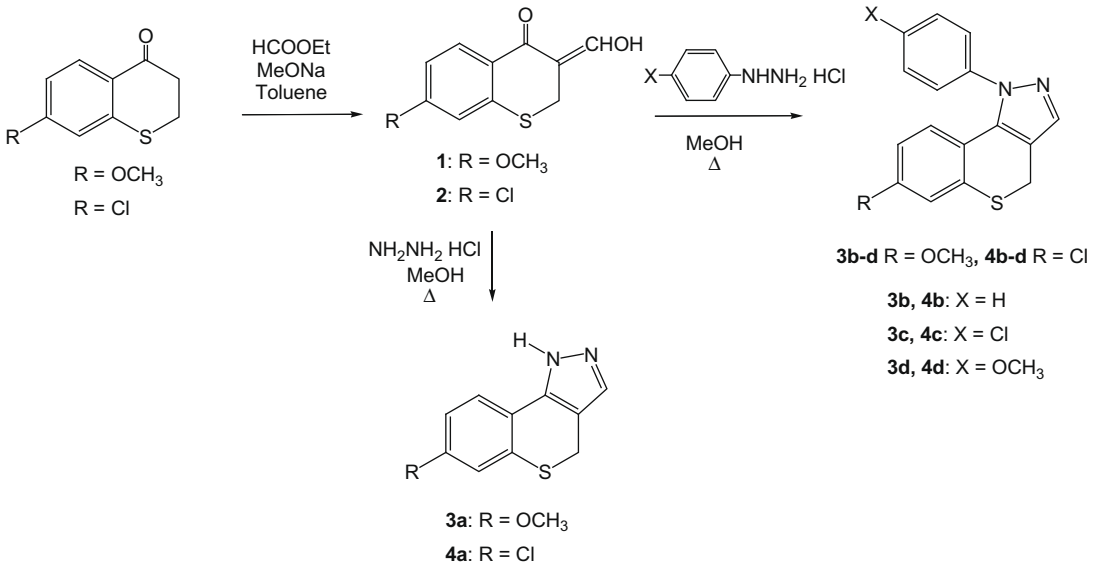

Scheme 1. Synthesis of 1-substituted-1,4-dihydrobenzothiopyrano[4,3-*c*]pyrazoles.

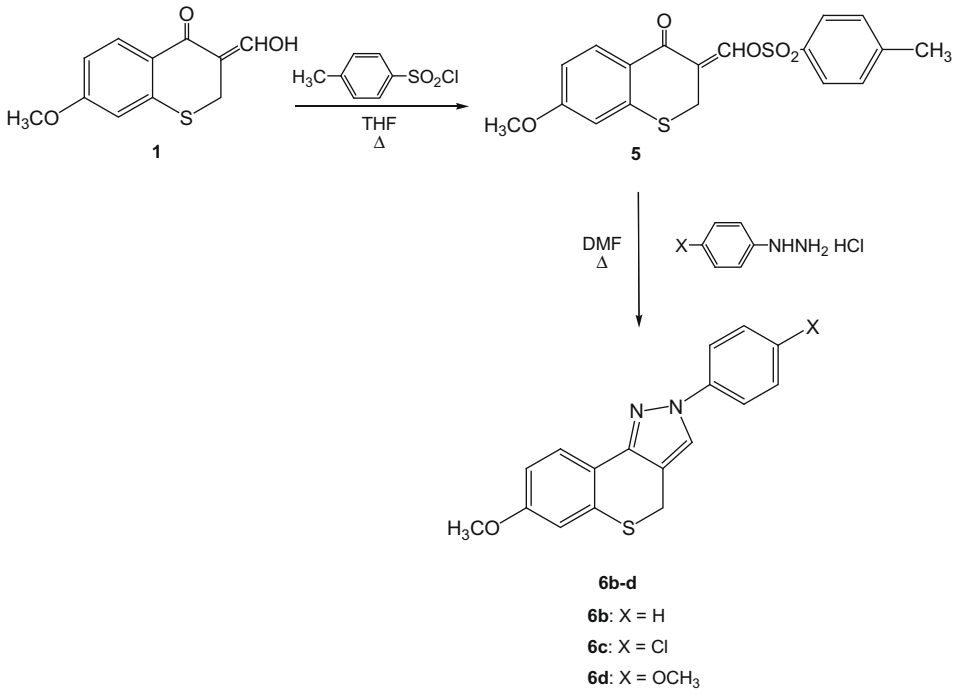

Scheme 2. Synthesis of 2-substituted-1,4-dihydrobenzothiopyrano[4,3-*c*]pyrazoles.

at the 1-position of the heterocyclic scaffold. Finally, a certain role seems to be played also by the methoxy substituent in position 7, indeed, its replacement with a chlorine (compounds **4b–d**) abolishes the biological activity.

2.3. Interaction with DNA

The presence of a heterocyclic chromophore suggested that the new benzothiopyranopyrazole derivatives **3b–d** could exert their antiproliferative effect because of a complexation with DNA, likely through an intercalative mode of binding. To verify the occurrence of an interaction with the macromolecule, flow linear dichroism (LD) experiments were performed. The spectra of an aqueous solution of salmon testes DNA alone (continuous line) and in the presence of **3c** (dashed line) are shown in Figure 1 as a representative example. In both spectra, a strong negative signal at 260 nm occurred, which is typical of the macromolecule, while at higher wavelengths, no further signal was detected.

Similar behaviors were also obtained for **3b** and **3d** (spectra not shown). Because the occurrence of a complexation with the DNA induces a LD signal at wavelengths higher than 260 nm, that is, in the spectral region where only the added chromophore can absorb,[22] it has to be concluded that the benzothiopyranopyrazole moiety was unable to form a complex with the macromolecule. Thus, the antiproliferative effect exerted by the new derivatives is attributable to a cellular target other than DNA.

Table 1
Cell growth inhibition in the presence of examined compounds.

Compound	IC_{50} (μM) of cell lines	
	HeLa	HL-60
3a	>20	>20
3b	17.2 ± 0.2	12.5 ± 0.3
3c	6.7 ± 0.4	3.8 ± 0.1
3d	17.8 ± 0.1	6.6 ± 0.5
4a	>20	>20
4b	>20	>20
4c	>20	>20
4d	>20	>20
6b	>20	>20
6c	>20	>20
6d	>20	>20

2.4. Effects on rat liver mitochondria (RLM)

As it is generally accepted, an important antiproliferative effect is played by the process of apoptosis, or programmed cell death, which would have the task of eliminating the abnormal cells. A prominent role in this process is exhibited by the mitochondria with the induction of the phenomenon of the inner membrane permeability transition (MPT), which provokes release in the cytosol of some factors, such as cyt *c*, AIF, and Smac DIABLO. These factors trigger the caspase-dependent and independent cascade, resulting in the apoptotic phenotype (for a review, see Ref. 3). In this regard, the main aim of this study is to evaluate the ability of compound **3c** to induce some effects on the mitochondrial functions ascribable to MPT induction. As reported in Figure 2A, when RLM, incubated in standard medium as described in Section 4, were treated with 50 μM **3c** in the presence of 30 μM Ca^{2+} an apparent decrease of approximately about 1 U in absorbance at 540 nm, was observed in the mitochondrial suspension. This event was indicative of the occurrence of a large-amplitude swelling at the mitochondrial matrix, furthermore, **3c** and Ca^{2+} were completely ineffective when incubated alone (Fig. 2A).

The colloid-osmotic swelling induced by **3c** was accompanied by a complete collapse of the electrical membrane potential ($\Delta\Psi$) (Fig. 2B) and ΔpH (result not reported), demonstrating that the compound induces a complete de-energization of the membrane. In both cases, the immunosuppressant CsA fully prevented the effects of **3c**.

The results reported in Figure 3A show that the mitochondrial swelling induced by **3c** in the presence of Ca^{2+} was prevented also by ADP, the alkylant agent NEM, and the AdNT inhibitor, BKA. All these inhibitors also completely hindered the collapse of $\Delta\Psi$, which was always induced by **3c** plus Ca^{2+} (Fig. 3B).

Taking into account that CsA, ADP, and BKA are typical inhibitors of the MPT and NEM is a protective agent against thiol oxidation,[23] the results of Figures 2 and 3 lead to the conclusion that **3c** behaves as an inducer of the transition pore opening and that its effect is most likely due to an oxidative stress provoked together with Ca^{2+}. This connection can be seen in the results reported in Figure 4.

Figure 4A shows the histogram regarding the changes in the redox level of the mitochondrial sulfydryl groups (SH) when the organelles were treated with **3c** and Ca^{2+}, either alone or together. The results demonstrate that both **3c** and Ca^{2+} when incubated alone decreased the total content of the SH groups by about 20%, but when incubated together, the decrease of the SH groups was doubled. These drops in the SH content account for a corresponding formation of oxidized dithiol groups. The strong inhibition of thiol oxidation exhibited by the reductant DTE further confirms that all the observed effects are the result of an oxidative stress. The results reported in Figure 4B also clarify that the above observed oxidative stress is due to hydrogen peroxide generation and most likely by its derivatives, in particular, the highly damaging hydroxyl radical which is produced by the interaction with the respiratory chain.[24,25] In fact, as observed in the figure, Ca^{2+} alone further incremented H_2O_2 production by the control (0.1 nmol/mg protein) up to 0.4 nmol/mg protein, while **3c** induced a minor increase of about 0.25 nmol/mg protein. Both agents lead to the generation of about 0.55 nmol/mg protein. The production of H_2O_2 by **3c** and Ca^{2+} was most likely attributable to a disorganization of the membrane phospholipids, resulting in an alteration of ubiquinone mobility and leading to reactive oxygen species (ROS) production.[26] In addition to the aforementioned effects, the increase in H_2O_2 production in the presence of both agents was due to the loss of the mitochondrial antioxidant systems, resulting in the so-called catastrophe redox that accompanies the opening of the pore.[27] However, it must be emphasized that the generation of ROS by Ca^{2+} was not involved in the oxidation of the critical SH groups responsible for pore opening, presumably because these ROS were formed away from the above thiols. Instead, the ROS formed by **3c**

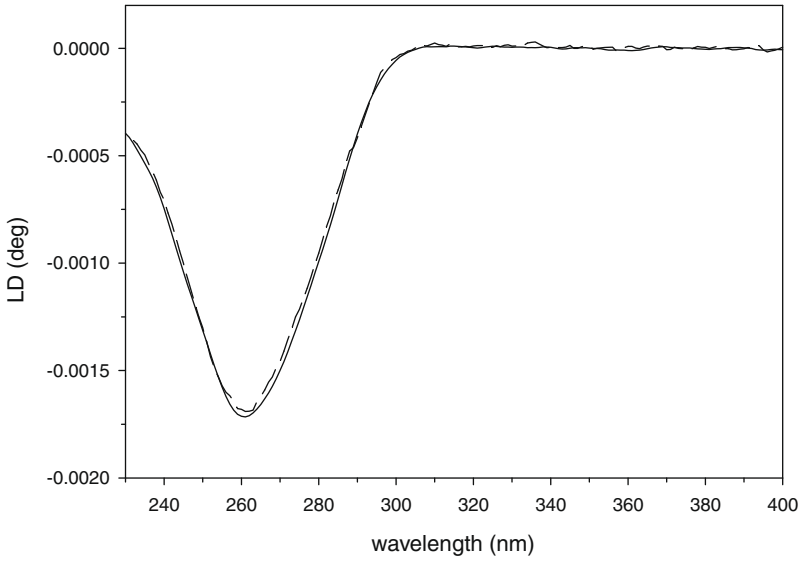

Figure 1. Linear flow dichroism spectra for DNA alone (continuous line) and in the presence of **3c** (dashed line) at [drug]/[DNA] = 0.08. [DNA] = 1.6×10^{-3} M.

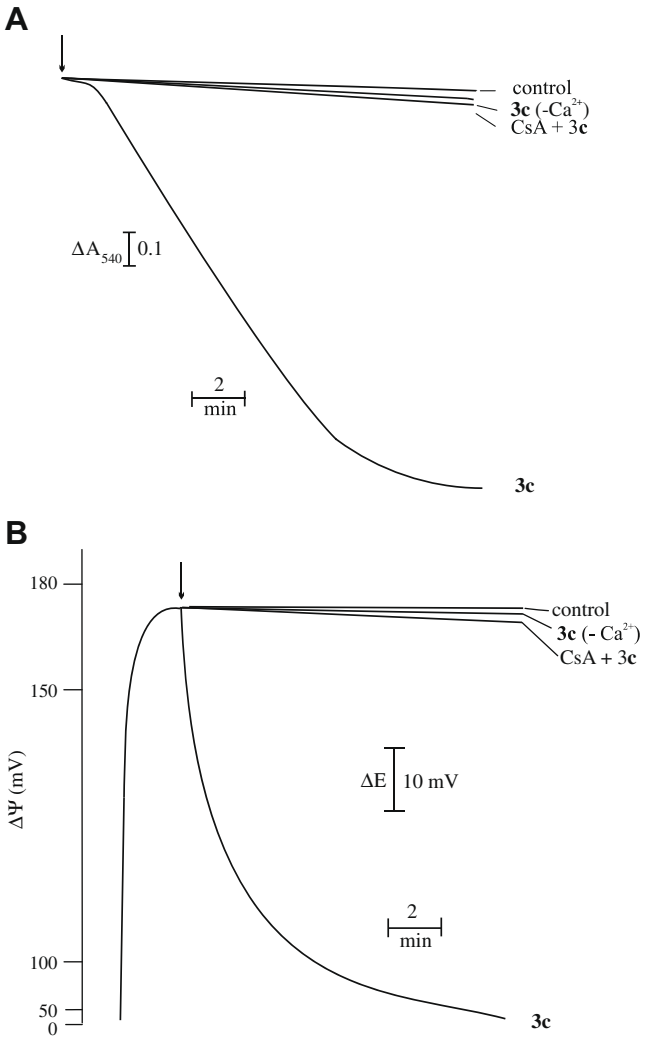

Figure 2. Effects of **3c** on mitochondrial swelling (A) and $\Delta\Psi$ collapse (B) and inhibition by CsA. All incubations were carried out as indicated in standard incubation procedures in the presence of 30 μ M Ca^{2+}, except where indicated (–Ca^{2+}). When present, the concentrations were 50 μM **3c** and 1 μM CsA. The assays were performed at least four times with similar results. (A) A downward deflection indicates absorbance decrease. (B) ΔE is the electrode potential.

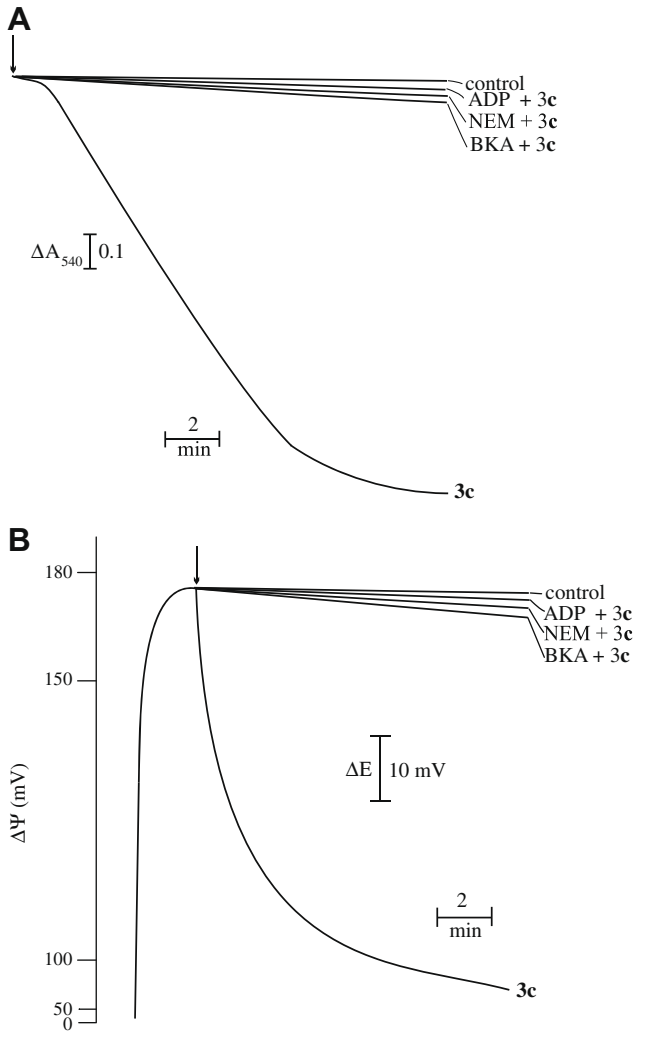

Figure 3. Effects of different MPT inhibitors on mitochondrial swelling (A) and $\Delta\Psi$ collapse (B) induced by **3c**. The experimental conditions are as indicated in the legend of Figure 2. When present, the concentrations were 1 mM ADP, 10 μM NEM, and 6 μM BKA. Data are representative of five similar experiments.

are strictly close to the critical sulfydryl groups located on AdNT.[28] It must be taken into account that **3c** required the presence of Ca^{2+} to open the pore because the cation favors the interaction of cyclophylin D with the pore forming structures which was necessary to induce this event.[29]

The correlation between the induction of MPT and apoptosis was demonstrated by the release of cyt *c* and AIF, as reported in Figure 5.

The immunoblot in Figure 5A shows that **3c** alone exhibited a negligible effect, as the control, in inducing cyt *c* efflux, while Ca^{2+} alone induced a consistent efflux of this protein. If present together both agents provoked the release of a very high amount of cyt *c*. Similar results are observable in the immunoblot showing AIF efflux (Fig. 5B). In conclusion, the release of the pro-apoptotic factors cyt *c* and AIF by **3c** in the presence of Ca^{2+} was consistent with the activation of both the caspase-dependent and caspase-independent signaling pathways, leading to apoptosis. This was confirmed by the complete inhibition of the mentioned factors exhibited by CsA. The observed release of both factors by Ca^{2+} alone was not due to mitochondrial swelling and outer membrane rupture as in the case with both agents (see Fig. 2A). Most likely, Ca^{2+} altered the phospholipid architecture of the outer membrane, broke the network of electrostatic bindings, which stabilizes both factors in the intermembrane space, and permitted their release. However, the released amount was not sufficient to trigger the apoptotic pathway, as demonstrated by the results reported below.

2.5. Evaluation of mitochondrial membrane potential on HeLa cells

In order to get information on the mitochondrial activity of whole HeLa cells, a flow cytometric study was carried out using JC-1, a fluorescent dye (Fig. 6). This probe is a monomeric molecule with green fluorescence (FL1, 530 nm emission after excitation at 488 nm), which is able to selectively enter the mitochondria driven by mitochondrial membrane potential. This uptake increases the concentration gradient of JC-1 leading to the formation of aggregates, which show high level of red fluorescence emission (FL2, 590 emission). In mitochondria undergoing a transition from polarized to depolarized potential JC-1 leaks out of the mitochondria into the cytoplasm as monomers resulting in a decrease of red fluorescence.

A signal FL2 emission of the control HeLa cells is shown in Figure 6A. The cells treated with 50 μM **3c** showed an evident

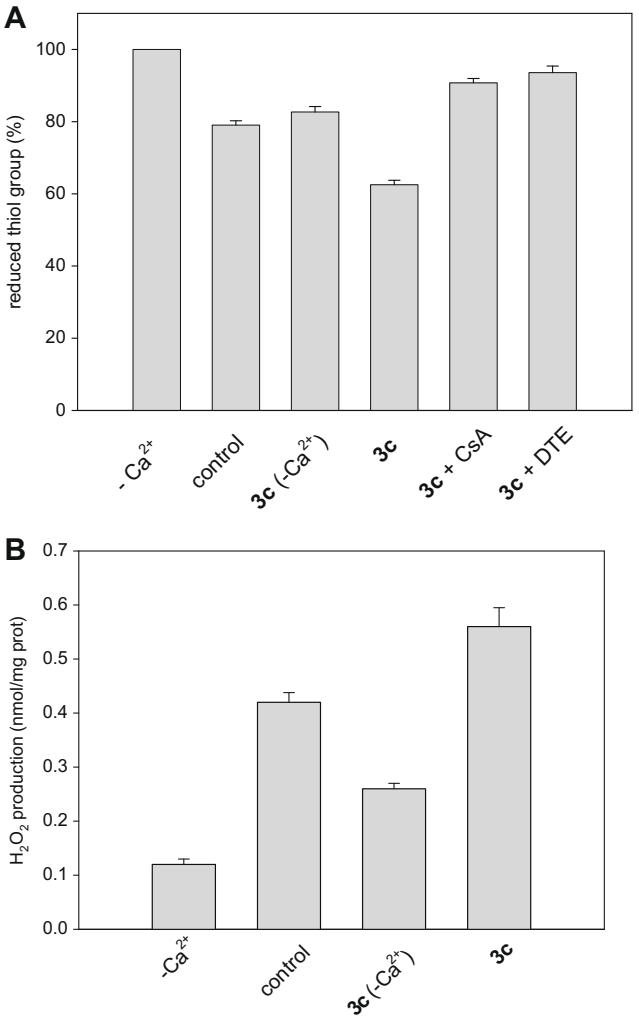

Figure 4. Mitochondrial thiol oxidation (A) and H_2O_2 production (B) induced by **3c**. All incubations were carried out as indicated in standard incubation procedures in the presence of 30 μM Ca^{2+}, except where indicated ($-Ca^{2+}$). When present, the concentrations were 50 μM **3c**, 1 μM CsA, and 2 mM DTE. The data represent average ± mean SD from four independent experiments.

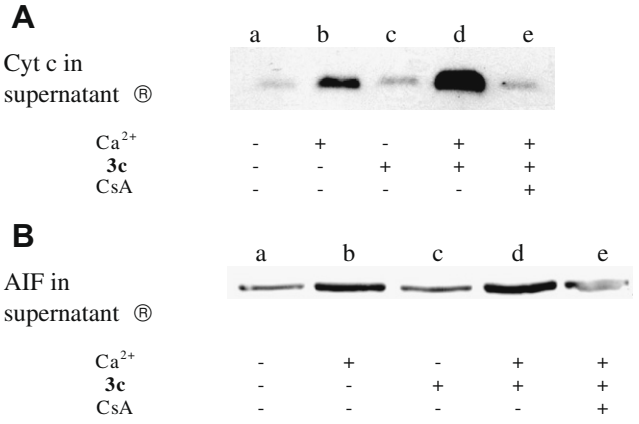

Fig. 5. Release of cytochrome *c* (cyt *c*) (A) and apoptosis-inducing factor (AIF) (B) induced by **3c** in the presence of Ca^{2+} and CsA. The result of the Western blotting of the supernatant fractions is shown. RLM were incubated in standard incubation procedures in the presence of 30 μM Ca^{2+}, except where indicated. When present, the concentrations were 50 μM **3c** and 1 μM CsA.

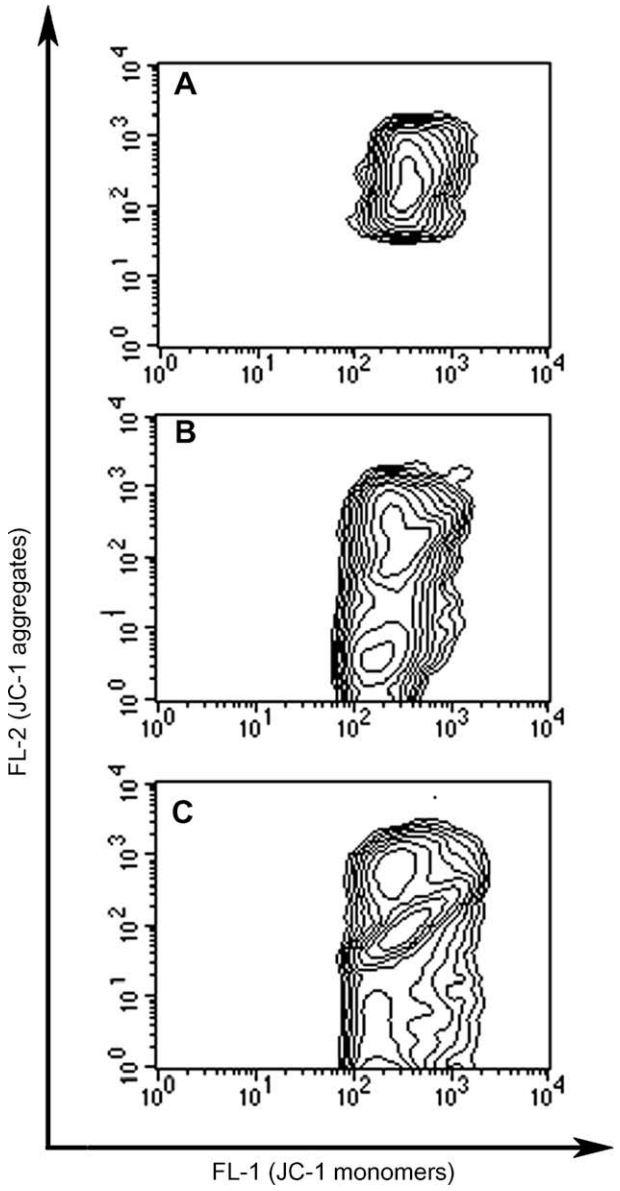

Figure 6. Mitochondrial membrane potential assessed by flow cytometry after JC-1 staining. Results are represented as contour plots. Control HeLa cells (A); cells treated with 50 μM **3c** (B) and with 20 μM H_2O_2 (C). A representative experiment of four is reported.

mitochondrial membrane depolarization, with a decreasing of the FL2 signal corresponding to 39.4% of the cellular population (Fig. 6B), as represented by the alterations of the contour plot. The cells with depolarized mitochondria are those from the middle of the quadrant to the lower right corner, as they lose greenish orange fluorescence (in FL2 channel).

Similar variations were also observed when the cells were incubated with exogenous H_2O_2. HeLa cells treated with a 20 μM exogenous hydrogen peroxide solution showed a mitochondrial membrane depolarization, corresponding to 20% of the cellular population (Fig. 6C).

2.6. Determination of apoptosis in HeLa cells

The release of cyt *c* in the cytoplasm led to the activation of the caspase cascade. Once activated, caspases become the effectors of cell death through the apoptotic process.

Apoptosis induction in HeLa cells, after treatment with **3c**, was evaluated by using Annexin V labeling (Fig. 7). Using DNA-specific viability dyes, such as PI, it was possible to distinguish early apoptotic cells (Annexin V-positive cells), late apoptotic cells (Annexin V- and PI-positive cells) and dead cells (PI-positive cells). After treatment with **3c** for 24 (Fig. 7B) and 48 (Fig. 7C) hours, an increase in apoptotic HeLa cells was observed, as revealed by Annexin V positivity of the early apoptotic fraction (19.7% and 8.5%, respectively) and late apoptotic fraction (28.2% and 39.0%, respectively) of cells. Moreover, a biochemical hallmark of apoptosis is the cleavage of chromosomal DNA into nucleosomal units that give rise to a 'ladder' of nucleosomal-sized multimers.[30] To evaluate whether the cell death induced by **3c** derived from mitochondrial-mediated apoptosis, we examined by gel electrophoresis the nuclear DNA extracted from HeLa cells treated with **3c** alone and after preincubation with CsA. Cells incubated in the presence of the well known drug cisplatin were taken as the reference. Figure 8 shows the typical DNA fragmentation which ensued from the activation of the apoptotic process for cells incubated with cisplatin (lane b) and with **3c** (lane c). The pre-treatment of HeLa cells with CsA clearly reduced the effect induced by **3c** (lane d).

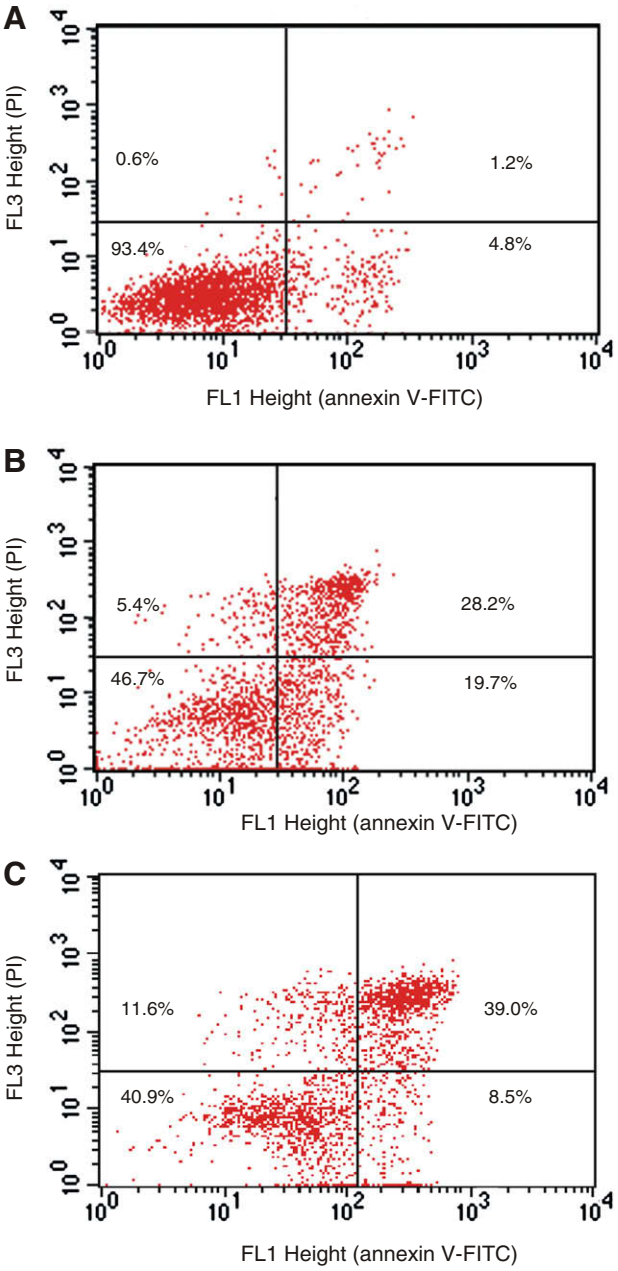

Figure 7. Dual parameter cytogram of FITC-labeled annexin V versus propidium iodide (PI) staining. Double-negative, non-apoptotic cells fall in the lower left quadrant, while early and late apoptosis cells fall in the lower and upper right quadrant, respectively. HeLa cells were incubated in the presence of 50 μM **3c** for 0 (A), 24 (B), and 48 (C) hours before staining.

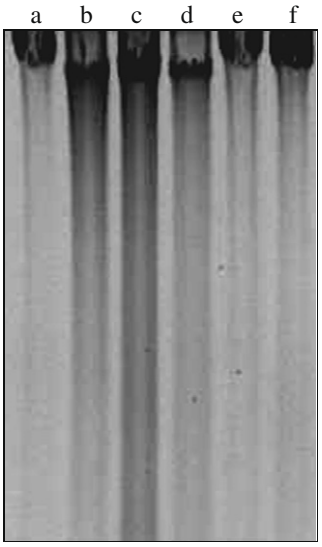

Figure 8. Agarose gel electrophoresis of DNA extracted from HeLa cells. Lane a, untreated control; lane b, 50 μM cisplatin; lane c, 100 μM **3c**; lane d, pre-treatment with 5 μM CsA for 30 min at 37 °C and then 100 μM **3c**; lane e, 5 μM CsA for 30 min at 37 °C; lane f, solvent alone.

These results indicate that the cell death provoked by **3c** was due to the initiation of intrinsic death signals that lead to apoptosis and that this latter process is strictly related to the induction of the opening of the mitochondrial permeability transition pore.

2.7. Cyclosporin A (CsA) antagonizes the antiproliferative effect on HeLa cells

To correlate the antiproliferative activity of **3c** (see Table 1) with the effects exerted on the mitochondria, HeLa cells were incubated in the standard medium containing Ca^{2+} and a cell inhibition growth assay was performed in the presence of CsA. Figure 9A shows the results, expressed in terms of the number of viable cells compared with the control cultures. Incubation of cells for 72 h with 6 μM **3c**, induced, as expected, a reduction in cell number of about 50% with respect to the untreated cells (control). According to the literature,[31] the pre-treatment with CsA alone (control + CsA) caused a certain cytotoxic effect and, indeed, a reduction in the cell number of about 20% with respect to the untreated cells, was observed. After the preincubation with CsA and the treatment with **3c**, approximately 64% of the viable cells were obtained (**3c** + CsA). Taking into account the above data, it was concluded that **3c**, at a concentration close to the IC_{50} value, induced a reduction in cell number of less than 20% after preincubation with CsA. Thus, CsA significantly reduced the antiproliferative effect of the test compound. The optical microphotographs shown in Figure 9B further confirm the above data.

3. Conclusions

The synthesis of a new heterocyclic benzothiopyranopyrazole nucleus, bearing a methoxy (**3a**) or a chlorine (**4a**) group in the

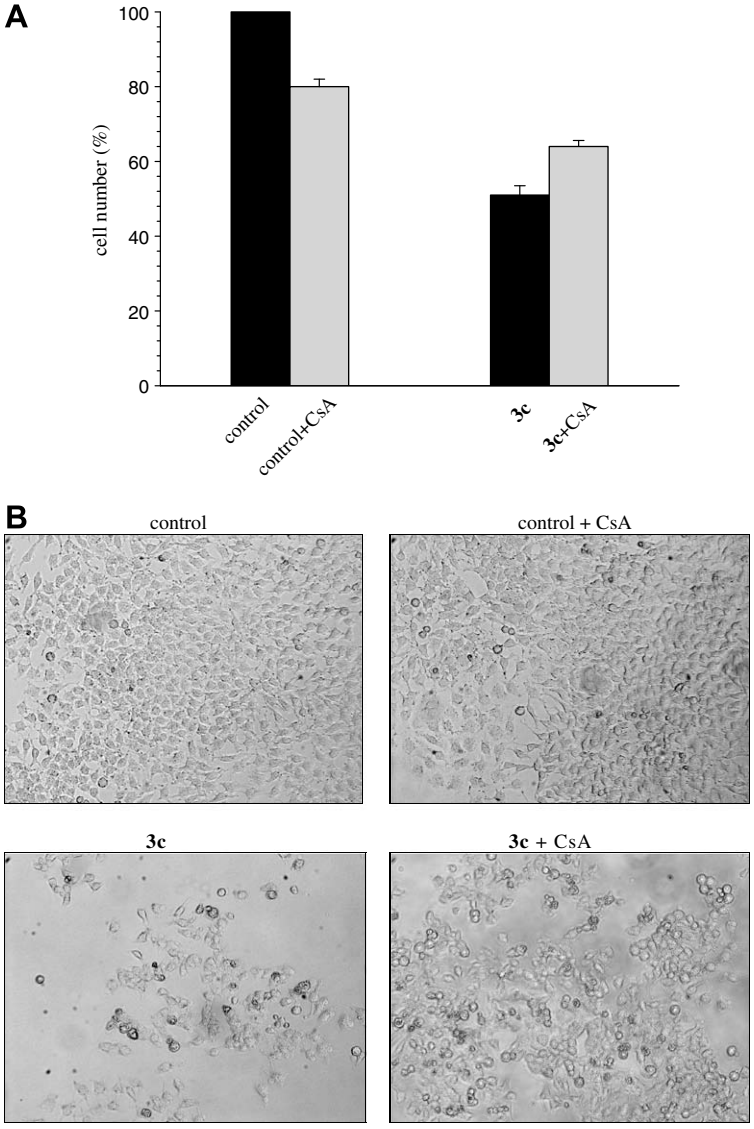

Figure 9. Effects of CsA on cell growth inhibition induced by **3c** evaluated as a percentage of cell number (A) and by optical microphotographs (B). HeLa cells were incubated for 72 h in the absence or in the presence of 6 μM **3c** as indicated, without pre-treatment (black bars) and after pre-treatment with 2 μM CsA for 30 min (grey bars).

7-position and a *p*-substituted phenyl either in the 1- (**3b–d** and **4b–d**) or in the 2-position (**6b–d**) of the pyrazole moiety, is described. Within this series of new derivatives, **3b–d** demonstrated the ability to inhibit cell growth and in particular, **3c** exhibited the higher cytotoxic capacity. These data pointed to the phenyl group in the 1-position of the pyrazole and the methoxy substituent in the 7-position of the benzothiopyranopyrazole nucleus as essential structural requirements for the occurrence of an antiproliferative effect. Investigation into the action mechanism of **3c** highlighted the absence of interaction with DNA. Interestingly, the new derivative acts as MPT inducer, causing a large-amplitude swelling of the mitochondrial matrix and the collapse of the electrical potential, both completely prevented by CsA, ADP, and BKA. The inhibitory effect of the alkylating agent NEM, along with the decrease in the total content of the SH groups, that accounts for a corresponding formation of oxidized dithiol groups, indicated that the mitochondrial events are the result of oxidative stress. Furthermore, the detection of an increase in the production of hydrogen peroxide reinforced this hypothesis. As a consequence of the opening of the permeability transition pore, **3c** provoked the release of the pro-apoptotic factors cyt *c* and AIF from the mitochondria, thus activating the caspase-dependent and caspase-independent apoptotic pathways, respectively. The HeLa cells treated with **3c** showed an evident mitochondrial membrane depolarization, similarly to that induced by H_2O_2 already described in the literature,[32] thus demonstrating that the effects measured on isolated mitochondria occur also in cells. Moreover, these results in whole cells confirm the above mentioned proposal that **3c** exhibits its effects by means of an oxidative stress. Phosphatidylserine exposure on the outer surface of the cytoplasmic membrane of HeLa cells clearly showed the onset of the apoptotic process and moreover, the nuclear DNA fragmentation, which characterizes cell death by apoptosis, was observed in the HeLa cells treated with **3c**. The link between the mitochondrial effects induced by **3c** and its antiproliferative activity emerges from the ability of CsA to prevent the cell death. In conclusion, the novel benzothiopyranopyrazole derivative **3c** activated the apoptotic pathway damaging mitochondrial functions, and this mechanism accounts for the antiproliferative effect on tumor cell lines. It should be noted that the ability to activate the apoptotic process by directly affecting mitochondria, along with the lack of interaction with DNA, represent interesting properties for the development of anticancer drugs. In

particular, the inability to form a complex with the macromolecule reduces the risk of genotoxicity. Furthermore, the mitochondrial targeted agents could play a crucial role in the attempt to overcome the chemoresistance acquired both as a consequence of the neutralization of pro-apoptotic signals that converge to mitochondria, like the loss of p53 expression, and the upregulation of anti-apoptotic proteins belonging to the Bcl-2 subfamily. Therefore, for these reasons, the benzothiopyranopyrazole nucleus constitutes a chromophore that should be further developed in an effort to obtain new improved anticancer therapies.

4. Experimental

4.1. Chemistry

4.1.1. Materials and methods

The uncorrected melting points were determined using a Reichert Köfler hot-stage apparatus. IR spectra were obtained on a NICOLET/AVATAR, 360 FT spectrophotometer by Nujol mulls. ^{1}H NMR spectra were recorded on a Varian Gemini 200 spectrometer in dimethyl-d_6 sulfoxide solution using TMS as the internal standard. The coupling constants are given in Hertz. Elemental analyses were performed by our Analytical Laboratory and were within ±0.4%. Magnesium sulfate was used as the drying agent. Evaporations were made in vacuo (rotating evaporator). Analytical TLC was carried out on Merck 0.2 mm precoated silica gel aluminum sheets (60 F-254). Reagents, starting materials, and solvents were purchased from commercial suppliers and used as received.

4.1.2. 7-Methoxy- and 7-chloro-2,3-dihydro-3-hydroxymethylene-1-benzothiopyran-4(4H)-one (1) and (2)

A solution of ethyl formate (1.25 mL, 15 mmol) in anhydrous toluene (6 mL) was added dropwise to freshly prepared sodium methoxide (0.345 g of sodium, 15 mmol, in 6 mL of absolute methanol) in the same solvent (8 mL). Then a solution of 7-methoxy- or 7-chloro-2,3-dihydro-4*H*-1-benzothiopyran-4-one, (7.5 mmol) in anhydrous toluene (10 mL) was added dropwise, with stirring, to the ice-cooled mixture, under a nitrogen atmosphere. Stirring was continued at room temperature for 24 h to give the sodium salt of **1** or **2**, which was collected and treated with water. The solution obtained was acidified with hydrochloric acid to give pure **1** (0.542 g, 48% yield) and **2** (1.546 g, 91% yield). An analytical sample was obtained by recrystallization from petroleum ether 30–60 °C.

Compound ***1***: mp 90–92 °C; ir: 1625, 1590, 1230, 1030 cm^{-1}; ^{1}H NMR: δ 3.81 (s, 3H, OCH_3); 3.82 (s, 2H, CH_2S); 6.82 (dd, 1H, 6-H J_{6-5} = 8.8 Hz J_{6-8} = 2.4 Hz); 6.89 (d, 1H, 8-H J_{8-6} = 2.4 Hz); 7.89 (d, 1H, 5-H J_{6-5} = 8.8 Hz). Anal. Calcd for $C_{11}H_{10}O_3S$: C, 59.46; H, 4.50. Found: C, 59.64; H, 4.49.

Compound ***2***: mp 102–104 °C; ir: 1640, 1580, 1105 cm^{-1}; ^{1}H NMR: δ 3.86 (s, 2H, CH_2S); 7.31 (dd, 1H, 6-H J_{6-5} = 8.5 Hz J_{6-8} = 2.1 Hz); 7.50 (d, 1H, 8-H J_{8-6} = 1.8 Hz); 7.91 (d, 2H, 5-H J_{6-5} = 8.6 Hz). Anal. Calcd for $C_{10}H_7ClO_2S$: C, 52.98; H, 3.09. Found: C, 52.80; H, 3.08.

4.1.3. 7-Methoxy-1,4-dihydro-benzothiopyrano[4,3-*c*]pyrazole (3a), 1-(*p*-substituted-phenyl)derivatives (3b–d), 7-chloro-1,4-dihydro-benzothiopyrano[4,3-*c*]pyrazole (4a) and 1-(*p*-substituted-phenyl)derivatives (4b–d)

General procedure: Hydrazine hydrochloride or the required phenylhydrazine hydrochloride (0.811 mmol) was added to a solution of **1** or **2** (0.676 mmol) in 15 mL of methanol, the reaction mixture was stirred at room temperature for 24 h and then refluxed for 15 h. After cooling, the yellow solid, if present, was collected and the solution was evaporated under reduced pressure. The solid and the residue were washed with an aqueous potassium carbonate solution to give crude pyrazoles **3a–d**, which were purified by recrystallization from ethanol, and **4a–d**, which were purified by flash chromatography on a silica gel column (60/0.040–0.063 mm) using petroleum ether 60–80 °C/ethyl acetate 8/2 as the eluting system.

Compound ***3a***: 38% yield; mp 154–156 °C; ir: 3300, 1600, 1480, 1250, 1100, 1035 cm^{-1}; ^{1}H NMR: δ 3.76 (s, 3H, OCH_3); 4.00 (s, 2H, CH_2-S); 6.80 (d, 1H, 8-H J_{8-9} = 8.4 Hz J_{8-6} = 2.6 Hz); 6.90 (d, 1H, 6-H J_{6-8} = 2.6 Hz); 7.56 (s, 1H, 3-H); 7.69 (d, 1H, 9-H J_{9-8} = 8.4 Hz). Anal. Calcd for $C_{11}H_{10}N_2OS$: C, 60.55; H, 4.59; N, 12.84. Found: C, 60.52; H, 4.60; N, 12.85.

Compound ***3b***: 39% yield; mp 105–108 °C; ir: 1600, 1510, 1280, 1225, 1035 cm^{-1}; ^{1}H NMR: δ 3.72 (s, 3H, OCH_3); 3.98 (s, 2H, CH_2-S); 6.59–6.62 (m, 2H, 6-H, 4′-H); 7.04 (d, 1H, 8-H J = 2.4 Hz); 7.35–7.39 (m, 2H, 2′-H, 6′-H); 7.51–7.54 (m, 3H, 3′-H, 5′-H, 9-H); 7.62 (s, 1H, 3-H). Anal. Calcd for $C_{17}H_{14}N_2OS$: C, 69.39; H, 4.76; N, 9.52. Found: C, 69.51; H, 4.78; N, 9.47.

Compound ***3c***: 47% yield; mp 127–129 °C; ir: 1600, 1500, 1290, 1225, 1040 cm^{-1}; ^{1}H NMR: δ 3.73 (s, 3H, OCH_3); 3.97 (s, 2H, CH_2-S); 6.67 (d, 1H, 8-H J_{8-9} = 2.4 Hz); 6.69 (s, 1H, 6-H); 7.05 (d, 1H, 9-H J_{9-8} = 2.4 Hz); 7.40 (d, 2H, 2′-H, 6′-H J = 8.6 Hz); 7.59 (d, 2H, 3′-H, 5′-H J = 8.6 Hz); 7.65 (s, 1H, 3-H). Anal. Calcd for $C_{17}H_{13}N_2OClS$: C, 62.10; H, 3.96; N, 8.52. Found: C, 62.15; H, 3.98; N, 8.53.

Compound ***3d***: 34% yield; mp 150–152 °C; ir: 1590, 1515, 1290, 1240, 1080, 1050 cm^{-1}; ^{1}H NMR: δ 3.71 (s, 3H, 7-OCH_3); 3.82 (s, 3H, 4′-OCH_3); 3.97 (s, 2H, CH_2-S); 6.61 (d, 1H, 8-H J_{8-9} = 2.4 Hz); 6.64 (s, 1H, 6-H); 7.02 (d, 1H, 9-H J_{9-8} = 2.4 Hz); 7.06 (d, 2H, 2′-H, 6′-H J = 8.8 Hz); 7.28 (d, 2H, 3′-H 5′-H J = 8.8 Hz); 7.56 (s, 1H, 3-H). Anal. Calcd for $C_{18}H_{16}N_2O_2S$: C, 66.66; H, 4.94; N, 8.64. Found: C, 66.97; H, 4.95; N, 8.62.

Compound ***4a***: 59% yield; mp 113–115 °C; ir: 3175; 1580; 1130 cm^{-1}; ^{1}H NMR: δ 4.05 (s, 2H, CH_2-S); 7.25 (d, 1H, 8-H J_{8-9} = 8.1 Hz); 7.41 (s, 1H, 3-H); 7,65 (s, 1H, 6-H); 7.77 (d, 1H, 9-H J_{9-8} = 8.1 Hz); 12.96 (s, 1H, NH exch.). Anal. Calcd for $C_{10}H_7N_2ClS$: C, 53.93; H, 3.15; N, 12.58. Found: C, 54.04; H, 3.14; N, 12.60.

Compound ***4b***: 20% yield; mp 98–103 °C; ir: 1595, 1500, 1070 cm^{-1}; ^{1}H NMR: δ 4.03 (s, 2H, CH_2-S); 6.68 (dd, 1H, 8-H J_{8-9} = 8.4 Hz J_{8-6} = 1.2 Hz); 7.08 (dt, 1H, 4′-H); 7.36–7.40 (m, 2H, ArH); 7.52–7.58 (m, 4H, ArH); 7.68 (d, 1H, 6-H J_{6-8} = 1.2 Hz). Anal. Calcd for $C_{16}H_{11}N_2ClS$: C, 64.32; H, 3.69; N, 9.38. Found: C, 64.37; H, 3.70; N, 9.39.

Compound ***4c***: 14% yield; mp 56–62 °C; ir: 1580, 1495, 1100 cm^{-1}; ^{1}H NMR: δ 4.02 (s, 2H, CH_2-S); 6.76 (d, 1H, 8-H J_{8-9} = 8.2 Hz); 7.15 (d, 1H, 9-H J_{9-8} = 8.2 Hz); 7.22 (s, 1H, 3-H); 7.42 (d, 2H, 3′-H 5′-H J = 8.4 Hz); 7.60 (d, 2H, 2′-H 6′-H J = 8.4 Hz); 7.71 (s, 1H, 6-H). Anal. Calcd for $C_{16}H_{10}N_2Cl_2S$: C, 57.66; H, 3.00; N, 8.41. Found: C, 57.70; H, 3.01; N, 8.43.

Compound ***4d***: 16% yield; mp 68–73 °C; ir: 1585, 1510, 1240, 1210 cm^{-1}; ^{1}H NMR: δ 3.80 (s, 3H, OCH_3); 4.12 (s, 2H, CH_2-S); 7.07 (d, 2H, 3′-H 5′-H J = 8.6 Hz); 7.29 (d, 1H, 8-H J_{8-9} = 8.2 Hz); 7.46 (s, 1H, 3-H); 7.76 (d, 2H, 2′-H 6′-H J = 8.6 Hz); 7.87 (d, 1H, 9-H J_{9-8} = 8.2 Hz); 8.31 (s, 1H, 6-H). Anal. Calcd for $C_{17}H_{13}N_2OSCl$: C, 62.10; H, 3.96; N, 8.52. Found: C, 62.13; H, 3.97; N, 8.51.

4.1.4. 3-[(*p*-Methylphenyl)sulfonyl]oxymethylen-2,3-dihydro-benzothiopyran-4(4*H*)-one (5)

p-Toluensulfonylchloride (3.960 g, 20.8 mmol) was added to a solution of **1** (2.310 g, 10.4 mmol) in 40 mL of anhydrous tetrahydrofurane in the presence of potassium carbonate (5.740 g, 41.6 mmol). The reaction mixture was stirred at room temperature for 24 h and then refluxed for 15 h. After cooling, the suspension was concentrated under reduced pressure and the residue obtained was treated with water and then extracted with chloroform. The organic layer was dried and evaporated to give crude product **5** which was purified by flash chromatography on a silica gel column

(60/0.040–0.063 mm) using petroleum ether 60–80 °C/ethyl acetate 7:3 as the eluting system. 68.8% yield: mp 73–75 °C; ir: 1670, 1480, 1300, 1260, 1230, 1180, 1140, 1090, 1050 cm^{-1}; ^1H NMR: δ 2.43 (s, 3H, CH_3); 3.81 (s, 3H, OCH_3); 3.90 (s, 2H, CH_2S); 6.84 (dd, 1H, 6-H J_{6-5} = 8.8 Hz J_{6-8} = 2.6 Hz); 6.90 (d, 1H, 8-H J_{8-6} = 2.6 Hz); 7.41 (s, 1H, CHO); 7.54 (d, 2H, 3′-H 5′-H J = 8.5 Hz); 7.92 (d, 1H, 5-H J_{5-6} = 8.8 Hz); 7.96 (d, 2H, 2′-H 6′-H J = 8.5 Hz). Anal. Calcd for $C_{18}H_{16}O_5S_2$: C, 57.45; H, 4.26. Found: C, 57.64; H, 4.27.

4.1.5. 7-Methoxy-2-(*p*-substituted-phenyl)-1,4-dihydrobenzothiopyrano[4,3-*c*] pyrazoles (6b–d)

General procedure: The required phenylhydrazine hydrochloride (2.4 mmol) was added to a solution of **5** (0.688 g, 2.00 mmol) in 10 mL of anhydrous dimethylformamide. The reaction mixture was stirred at room temperature for 24 h and then refluxed at 100 °C for 15 h. After cooling, the suspension was poured into water and then extracted with chloroform. The organic layer was dried and evaporated under reduced pressure to give desired crude pyrazoles **6b–d**, which were purified by flash chromatography on a silica gel column (60/0.040–0.063 mm) using petroleum ether 60–80 °C/ethyl acetate 8:2 as the eluting system.

*Compound **6b**:* 45% yield; mp 110–115 °C; ir: 1600, 1500, 1300, 1250, 1220, 1035 cm^{-1}; ^1H NMR: δ 3.78 (s, 3H, OCH_3); 4.09 (s, 2H, CH_2-S); 6.85 (dd, 1H, 8-H J_{8-9} = 8.5 Hz J_{8-6} = 2.6 Hz); 6.94 (d, 1H, 6-H J_{6-8} = 2.6 Hz); 7.30 (t, 1H, 4′-H J = 7.3 Hz); 7.50 (t, 2H, 3′-H 5′-H J = 7.6 Hz); 7.83 (d, 1H, 9-H J_{9-8} = 8.5 Hz); 7.85 (d, 2H, 2′-H 6′-H J = 7.6 Hz); 8.37 (s, 1H, 3-H). Anal. Calcd for $C_{17}H_{14}N_2OS$: C, 69.39; H, 4.76; N, 9.52. Found: C, 69.44; H, 4.77; N, 9.51.

*Compound **6c**:* 30% yield; mp 88–93 °C; ir: 1600, 1500, 1245, 1095, 1050 cm^{-1}; ^1H NMR: δ 3.78 (s, 3H, OCH_3); 4.08 (s, 2H, CH_2-S); 6.84 (dd, 1H, 8-H J_{8-9} = 8.6 Hz J_{8-6} = 2.6 Hz); 6.94 (d, 1H, 6-H J_{6-8} = 2.6 Hz); 7.56 (d, 2H, 2′-H 6′-H J = 9.0 Hz); 7.83 (d, 1H, 9-H J_{9-8} = 8.6 Hz); 7.88 (d, 2H, 3′-H 5′-H J = 9.0 Hz); 8.40 (s, 1H, 3-H). Anal. Calcd for $C_{17}H_{13}N_2OClS$: C, 62.10; H, 3.96; N, 8.52. Found: C, 62.00; H, 3.98; N, 8.54.

*Compound **6d**:* 31% yield; mp 108–112 °C; ir: 1600, 1510, 1300, 1245, 1050 cm^{-1}; ^1H NMR: δ 3.78 (s, 3H, OCH_3); 3.80 (s, 3H, OCH_3); 4.07 (s, 2H, CH_2-S); 6.83 (dd, 1H, 8-H J_{8-9} = 8.6 Hz J_{8-6} = 2.6 Hz); 6.93 (d, 1H, 6-H J_{6-8} = 2.6 Hz); 7.06 (d, 2H, 2′-H 6′-H J = 9.0 Hz); 7.75 (d, 2H, 3′-H 5′-H J = 9.0 Hz); 7.80 (d, 1H, 9-H J_{9-8} = 8.6 Hz); 8.25 (s, 1H, 3-H). Anal. Calcd for $C_{18}H_{16}N_2O_2S$: C, 66.66; H, 4.94; N, 8.64. Found: C, 66.73; H, 4.95; N, 8.67.

4.2. Biology

4.2.1. Cell cultures

HL-60 (human myeloid leukemic) and HeLa (human cervix adenocarcinoma) cells were grown in RPMI 1640 (Sigma Chemical Co.) supplemented with 15% heat-inactivated fetal calf serum (Biological Industries) and in Nutrient Mixture F-12 [HAM] (Sigma Chemical Co.) supplemented with 10% heat-inactivated fetal calf serum (Biological Industries). One hundred U/mL penicillin, 100 μg/mL streptomycin, and 0.25 μg/mL amphotericin B (Sigma Chemical Co.) were added to both media. The cells were cultured at 37 °C in moist atmosphere of 5% carbon dioxide in air.

4.2.2. Inhibition growth assays

HL-60 cells (4×10^4) were seeded into each well of a 24-well cell culture plate. After incubation for 24 h, various concentrations of the test agents were added to the complete medium and incubated for another 72 h. HeLa (4×10^4) cells were seeded into each well of a 24-well cell culture plate. After incubation for 24 h, the medium was replaced with an equal volume of fresh medium, and various concentrations of the test agents were added. The cells were then incubated in standard conditions for another 72 h. A trypan blue assay was performed to determine cell viability. Cytotoxicity data were expressed as IC_{50} values, that is, the concentration of the test agent inducing 50% reduction in cell number compared with the control cultures.

For the experiments in the presence of CsA, after incubation for 24 h, the HeLa cells were treated with 2 μM CsA for 30 min; the medium was replaced with an equal volume of fresh medium, 6 μM of test agent was added, and the cells were incubated for another 72 h. Cell viability was determined by a trypan blue assay and expressed as a percentage of the cell number of control culture. For the microphotographs, cell cultures were washed with PBS buffer, fixed with 3.7% formaldehyde in PBS, and then examined under an optical microscope (Leitz DMIRB, Leica).

4.2.3. Linear flow dichroism

Linear dichroism (LD) measurements were performed on a Jasco J500A circular dichroism spectropolarimeter converted for LD and equipped with an IBM PC and a Jasco J interface.

Linear dichroism is defined as

$$LD_{(\lambda)} = A_{//(\lambda)} - A_{\perp(\lambda)}$$

where $A_{//}$ and $A\perp$ correspond to the absorbances of the sample when polarized light is oriented parallel or perpendicular to the flow direction, respectively. The orientation is produced by a device designed by Wada and Kosawa[33] at a shear gradient of 500–700 rpm and each spectrum was acquired four times.

Salmon testes DNA was purchased from Sigma Chemical Co. (D-1626). The DNA concentration was determined using an extinction coefficient of 6600 $M(p)^{-1}$ cm^{-1} at 260 nm. A solution of salmon testes DNA (1.6×10^{-3} M) in ETN buffer (containing 10 mM Tris, 10 mM NaCl, and 1 mM EDTA, pH 7) was used. Spectra were recorded at 25 °C at [drug]/[DNA] = 0.00 and 0.08.

4.2.4. Mitochondrial isolation and standard incubation procedures

Rat liver mitochondria (RLM) were isolated by conventional differential centrifugation in a buffer containing 250 mM sucrose, 5 mM Hepes (pH 7.4), and 1 mM EGTA[34] the EGTA was omitted from the final washing solution. The protein content was measured by the biuret method with BSA as a standard.[35]

The mitochondria (1 mg protein/mL) were incubated in a water-jacketed cell at 20 °C. The standard medium contained 250 mM sucrose, 10 mM Hepes (pH 7.4), 5 mM succinate, and 1.25 μM rotenone. Variations and/or other additions were given with each experiment.

4.2.5. Determination of mitochondrial functions

The membrane potential ($\Delta\Psi$) was calculated on the basis of distribution of the lipid-soluble cation tetraphenylphosphonium (TPP^+) measured across the inner membrane using a TPP^+-specific electrode.[36] The mitochondrial swelling was determined by measuring the apparent absorbance change of the mitochondrial suspensions at 540 nm in a Kontron Uvikon model 922 spectrophotometer equipped with thermostatic control. The protein sulfydryl oxidation assay was performed as in Santos et al.[37] The production of H_2O_2 in RLM was measured fluorometrically by the scopoletin method[38] in a 4-8202 spectrofluorometer (Aminco-Bowman, Silver Spring, MD).

4.2.6. Detection of cyt *c* and AIF release

The mitochondria (1 mg protein/mL) were incubated for 15 min at 20 °C in standard medium with the appropriate additions. The reaction mixtures were then centrifuged at 13,000 g for 10 min at 4 °C to obtain mitochondrial pellets. The supernatant fractions were concentrated using a PAGEprep™ protein clean-up and enrichment kit (Pierce, Rockford, IL). Aliquots of 20 μL of the con-

centrated supernatants were subjected to 15% and 10% SDS–PAGE for cyt *c* and AIF, respectively, and analyzed by Western blotting using mouse anti-cyt *c* and rabbit anti-AIF antibodies (Pharmingen, San Diego, CA).

4.2.7. Determination of mitochondrial membrane potential on whole HeLa cells

The mitochondrial membrane potential was evaluated by using the lipophilic cationic probe 5,5′,6,6′-tetrachloro-1,1′,3,3′-tetraethylbenzimidazolcarbocyanine iodide (JC-1, Molecular Probes) according to Cossarizza et al.[39] HeLa cells were grown to near confluence, were treated with 50 μM **3c** in DMSO and then were incubated for 24 h at 37 °C. In the last 10 min of treatment, JC-1 was added at a final concentration of 5 ng/ml. As positive controls, HeLa cells were treated with a 20 μM exogenous hydrogen peroxide solution (commercial H_2O_2, Baker Analysed Reagent, J.T. Baker, Deventer, The Netherlands) for 24 h and then labeled as described above.

After washing with cold PBS, all the samples (10^5/ml cells) were analyzed by a FACScan flow cytometer (Becton–Dickinson, Mountain View, CA) equipped with a 15 mW, 488 nm, air-cooled argon ion laser. The fluorescence emissions attributed to JC-1 monomers was collected through a 530 nm band-pass filter, while the fluorescent signals ascribed to JC-1 aggregates were collected through the 585 and 650 nm band-pass filters, respectively. At least 10,000 events per each sample were acquired in log mode. Results are presented as percentages calculated by using the Cell Quest software (Becton–Dickinson).

4.2.8. Evaluation of apoptotic cell death by Annexin V-FITC staining

To detect phosphatidylserine translocation from the inner face to the outer surface of plasma membrane in the initialling step of apoptosis, an Annexin V-FITC kit (MBL, Medical & Biological Laboratories Co., Ltd, Japan) was used.[40] About 50 phosphatidylserine monomers are estimated to be bounded per Annexin V molecule.

HeLa cells were grown to near confluence, treated with 50 μM test compound and then were incubated for 24 and 48 h at 37 °C. After treatment, cells were centrifuged and resuspended in binding buffer (10 mM Hepes/NaOH, pH 7.5, 140 mM NaCl, and 2.5 mM $CaCl_2$). Cell suspensions (of about 5×10^5) were then incubated with 1 μg/ml of Annexin V-FITC and with 1 μg/ml of propidium iodide (PI) for 10 min at room temperature in the dark. The populations of Annexin V-positive/PI-negative cells (early apoptosis) and Annexin V-positive/PI-positive cells (late apoptosis) were evaluated by flow cytometry.[40] The reported values are the mean of three independent experiments.

4.2.9. DNA isolation and electrophoresis

HeLa cells (5×10^5) were incubated in standard conditions for 24 h at 37 °C and then, where indicated, incubated for 30 min at 37 °C with 5 μM CsA. The medium was then replaced with an equal volume of fresh medium and the test agent was added at the indicated concentration. After 24 h, DNA was extracted from the cells according to the procedure described by Sambrook et al.[41] The isolated DNA was dissolved in TE buffer (Tris 10 mM, pH 8, EDTA 1 mM) and analyzed by agarose (0.8%) gel electrophoresis in TBE buffer (Tris 0.09 M, EDTA 2 mM, boric acid 0.09 M, pH 8). The gel was stained with ethidium bromide solution (1 μg/mL) and then transilluminated by UV light and fluorescence emission visualized using a CCD camera coupled to a Bio-Rad Gel Doc 1000 apparatus.

Acknowledgment

This work was supported by grants from MIUR (Research fund Cofin 2006).

References and notes

1. Szewczyk, A.; Wojtczak, L.. *Pharmacol. Rev.* **2002**, *54*, 101.
2. Dias, N.; Bailly, C. *Biochem. Pharmacol.* **2005**, *70*, 1.
3. Kroemer, G.; Galluzzi, L.; Brenner, C. *Physiol. Rev.* **2007**, *163*, 87.
4. Green, DR.; Reed, JC. *Science* **1998**, *281*, 1309.
5. Ashkenazi, A. *Science* **1998**, *281*, 1305.
6. Jung, K.; Reszka, R. *Adv. Drug Delivery Rev.* **2001**, *49*, 87.
7. Huigsloot, M.; Tijdens, I. B.; Mulder, G. I.; van de Water, B. *J. Biol. Chem.* **2002**, *277*, 35869.
8. Tao, Z.; Withers, H. G.; Penefsky, H. S.; Goodisman, J.; Souid, A. *Chem. Res. Toxicol.* **2006**, *19*, 1051.
9. Munteanu, E.; Verdier, M.; Grandjean-Forestier, F.; Stenger, C.; Jayat-Vignoles, C.; Huet, S.; Robert, J.; Ratinaud, M.-H. *Biochem. Pharmacol.* **2006**, *71*, 1162.
10. Gong, Y.; Wang, Y.; Chen, F.; Han, J.; Miao, J.; Shao, N.; Fang, Z.; Ou Yang, R. *Leukocyte Res.* **2000**, *24*, 769.
11. Lin, J. H.; Castora, F. J. *Biochem. Biophys. Res. Commun.* **1991**, *176*, 690.
12. Robertson, J. D.; Gogvadze, V.; Zhivotovsky, B.; Orrenius, S. *J. Biol. Chem.* **2000**, *275*, 32438.
13. Karpinich, N. O.; Tafani, M.; Schneider, T.; Russo, M. A.; Farber, J. L. *J. Cell. Physiol.* **2006**, *208*, 55.
14. Da Settimo, A.; Marini, A. M.; Primofiore, G.; Da Settimo, F.; Salerno, S.; Viola, G.; Dalla Via, L.; Marciani Magno, S. *Eur. J. Med. Chem.* **1998**, *33*, 685.
15. Da Settimo, A.; Marini, A. M.; Primofiore, G.; Da Settimo, F.; Salerno, S.; Dalla Via, L.; Gia, O.; Marciani Magno, S. *Farmaco* **2001**, *56*, 159.
16. Dalla Via, L.; Gia, O.; Marciani Magno, S.; Da Settimo, A.; Primofiore, G.; Da Settimo, F.; Simorini, F.; Marini, A. M. *Eur. J. Med. Chem.* **2002**, *37*, 475.
17. Dalla Via, L.; Marini, A. M.; Salerno, S.; Toninello, A. *Biochem. Pharmacol.* **2006**, *72*, 1657.
18. Marini, A. M.; Da Settimo, F.; Salerno, S.; La Motta, C.; Simorini, F.; Taliani, S.; Bertini, D.; Gia, O.; Dalla Via, L. *J. Heterocycl. Chem.* **2008**, *45*, 745.
19. Degani, I.; Fochi, R.; Spunta, G. *Bollettino Scientifico della Facolta di Chimica Industriale di Bologna* **1966**, *24*, 75; . *Chem. Abstr* **1967**, *66*, 46292.
20. Primofiore, G.; Marini, A. M.; Da Settimo, F.; Salerno, S.; Bertini, D.; Dalla Via, L.; Marciani Magno, S. *J. Heterocycl. Chem.* **2003**, *40*, 783.
21. Primofiore, G.; Marini, A. M.; Salerno, S.; Da Settimo, F.; Bertini, D.; Dalla Via, L. *J. Heterocycl. Chem.* **2005**, *42*, 1357.
22. Nordén, B.; Kurucsev, T. *J. Mol. Recognit.* **1994**, *7*, 141.
23. Zoratti, M.; Szabò, I. *Biochim. Biophys. Acta* **1995**, *1241*, 139.
24. Battaglia, V.; Salvi, M.; Toninello, A. *J. Biol. Chem.* **2005**, *280*, 33864.
25. Cao, G.; Sofic, F.; Prior, R. L. *Free Radical Biol. Med.* **1997**, *22*, 749.
26. Grijalba, M. T.; Vercesi, A. E.; Schreier, S. *Biochemistry* **1999**, *38*, 13279.
27. Susin, S. A.; Zamzami, N.; Kroemer, G. *Biochim. Biophys. Acta* **1998**, *1366*, 151.
28. McStay, G. P.; Clarke, S. J.; Halestrap, A. P. *Biochem. J.* **2002**, *367*, 541.
29. Halestrap, A. P.; Davidson, A. M. *Biochem. J.* **1990**, *268*, 153.
30. Wyllie, A. H. *Nature (London)* **1980**, *284*, 555.
31. Ito, C.; Ribeiro, R. C.; Behm, F. G.; Raimondi, S. C.; Pui, C.-H.; Campana, D. *Blood* **1998**, *91*, 1001.
32. Arancia, G.; Calcabrini, A.; Marra, M.; Crateri, P.; Artico, M.; Martone, A.; Martelli, F.; Agostinelli, E. *Amino Acids* **2004**, *26*, 273.
33. Wada, A.; Kozawa, S. *J. Polym. Sci. Part A* **1964**, *2*, 853.
34. Schneider, W. C.; Hogeboom, G. H. *J. Biol. Chem.* **1950**, *183*, 123.
35. Gornall, A. G.; Bardawill, C. J.; David, M. M. *J. Biol. Chem.* **1949**, *177*, 751.
36. Kamo, N.; Muratsugu, M.; Hongoh, R.; Katabake, Y. *J. Membr. Biol.* **1979**, *49*, 105.
37. Santos, A. C.; Uyemura, S. A.; Lopes, J. L. C.; Bazon, J. N.; Minigatto, F. E.; Curti, C. *Free Radical Biol. Med.* **1998**, *24*, 1455.
38. Loschen, G.; Azzi, A.; Flohè, L. *FEBS Lett.* **1973**, *33*, 84.
39. Cossarizza, A.; Baccarani-Contri, M.; Kalashnikova, G.; Franceschi, C. *Biochem. Biophys. Res. Commun.* **1993**, *197*, 40.
40. van Engeland, M.; Nieland, L. J.; Ramaekers, F. C.; Schutte, B.; Reutelingsperger, C. P. *Cytometry* **1998**, *31*, 1.
41. Sambrook, J.; Fritsch, E. F.; Maniatis, T. Analysis and Cloning of Eucaryotic Genomic DNA. In *Molecular Cloning: A Laboratory Manual*; Nolan, C., Ed., 2nd ed.; Cold Spring Harbor Laboratory Press: Cold Spring Harbor, NY, 1989; pp 9.14–9.16.